Microglial depletion worsens lesion in female but not male C57BL/6J mice after P10 hypoxia-ischemia

Danielle Guez-Barber[1,2]*, Sofia Nicolayevsky[1], Kaya J.D. Johnson, Sanghee Yun[2,3], Amelia J. Eisch[3,4]

[1]Division of Neurology, The Children's Hospital of Philadelphia (CHOP), Philadelphia, PA, USA, 19104
[2]University of Pennsylvania Perelman School of Medicine, Philadelphia, PA, USA, 19104
[3]Department of Anesthesiology and Critical Care Medicine, CHOP Research Institute, Philadelphia, PA, USA, 19104
[4]Department of Neuroscience, University of Pennsylvania Perelman School of Medicine, Philadelphia, PA, USA, 19104

*Correspondence: barberd2@chop.edu

Pre-Submission Author Contributions (for details and explanations see CRediT):
Listed in alphabetical order by last name
Conceptualization: DGB
Data curation: DGB, SNG
Formal Analysis: DGB, SNG
Funding acquisition: DGB, AJE
Investigation: DGB, SNG, KJJ
Methodology: DGB, SNG, KJJ
Project administration: DGB
Resources: DGB, SY, AJE
Software: --
Supervision: DGB, SY, AJE
Validation: DGB, SNG
Visualization: DGB, SNG, SY, AJE
Writing, original draft: DGB, SNG
Writing, review & editing: DGB, SY, AJE

Acknowledgements: We would like to thank: Oscar Marcos-Contreras and Raul Chavez-Valdez for teaching DGB how to perform HI; Sheyenne Gillis for assistance setting up the HI model and collecting data for first cohort of HI mice; Ida Narli for assistance with Iba1 signal quantification in PLX-HI cohort; Mariko Bennett, F. Chris Bennett and Sonia Lombroso for helpful discussions about microglia depletion; Fred Kiffer, Lorianna Colon and Ruthie Wittenberg for suggestions on improving the manuscript and clarity of figures; Rui Xiao, Antoneta Karaj and Gabrielle Gionet for statistical guidance. DGB is supported by NIH CNCDP-K12 NS098482, CHOP Research Institute (K-Readiness Pilot Award; Foerderer Award), and the CHOP Division of Neurology. AJE is supported by NASA, NIH, CHOP, and philanthropic funds.

ABSTRACT

Background: Rodent models for perinatal hypoxic ischemic (HI) encephalopathy have reported sex differences such as males having larger brain lesions than females after the same injury. Microglia, the resident immune cells of the brain that have distinct developmental trajectories and gene expression patterns by sex, likely play a different role in males and females following HI. However, there is conflicting literature on whether depletion of microglia worsens or improves HI-induced lesions, and whether this differs by sex. We tested the effect of pharmacologic microglial depletion on lesion size and developmental milestones.
Methods: C57BL/6J mouse pups received daily intraperitoneal injections from postnatal day 7 (P7) to P12 of either 25 mg/kg PLX3397 (a CSF1R inhibitor) or vehicle (Veh). At P10, pups either underwent Hypoxic-Ischemic (HI) insult using a modified Vannucci procedure, or a Sham insult. This resulted in four groups tested (Veh-Sham, Veh-HI, PLX-Sham, PLX-HI); all groups included both male and female mice. Behavioral testing was performed both pre-HI (forelimb grasping [P8, P9]) and post-HI (open field traversal [P12], gross behavior and appearance in homecage and new environment [P13]). Brains were collected at P13, fixed, and sectioned, then either immunolabeled for Iba1 or stained with cresyl violet for injury scoring.
Results: Immunohistochemistry for Iba1 demonstrated >95% depletion of microglia at either P10 or P13 in all PLX3397-treated mice; depletion did not differ by sex. In the hippocampus, Female PLX-HI mice had worse cresyl violet lesion scores than Female Veh-HI mice; this was not true in male mice, where there was a trend in the opposite direction. Female PLX-HI mice also had worse lesion scores than Male PLX-HI mice. There were no differences among groups in forelimb grasp, open field traversal times, or weight gain.
Conclusion: Microglial depletion worsens HI-induced injury in female mice but not in male mice.

Keywords: microglia, hypoxic-ischemic encephalopathy, neonate, sex differences

INTRODUCTION

Perinatal hypoxic ischemic encephalopathy (HIE) is among the most common causes of death and disability in neonates globally.[1–3] Many studies in perinatal HIE animal models report distinct outcomes by sex. For example, male mice have larger lesions than female mice after the same injury and perform worse than females on a hippocampal-dependent task.[4] In fact, male rodents generally show larger anatomic injuries[4–6] and worse cognition[7,8] after HI relative to female rodents. The sex-specific differences are not limited to cognitive effects. Rats undergoing the same hypoxic injury show sex-dependent motor outcomes; males present a more spastic phenotype and females present a more dystonic phenotype.[9] Even treatment approaches need to be assessed for their sex-specific effects. For example, while hypothermia reduces HIE injury in humans and HI injury in rodents, analysis of the effect in rodents revealed that therapeutic hypothermia is actually beneficial in female, but not male, rodents.[10] Overall, these and many other studies underscore the critical importance of reporting and considering sex in HI studies.

Many factors may contribute to the sex-dependent response to perinatal HI, including sex differences in brain development,[11–13] cell death,[14–16] metabolism,[17] and immune function.[18–23] One established factor mediating sex differences in stroke[24] and other pathologies[25,26] — but understudied in perinatal HI — is microglia. In healthy brains, microglia (immune cells native to the brain[27,28]) orchestrate developmental pruning of synapses,[29–31] shape cellular indices of learning,[32,33] and regulate behavior,[34,35] including sex-specific behavior.[25,27,36] Microglia are different in males and females; they have sex-dependent developmental trajectories[34,37–39] and gene expression patterns.[40,41] Lesion[42,43] and transplantation[24] studies show microglia play different roles in male and female brains after HI or stroke. However, there are conflicting data on whether microglial depletion prior to HI or stroke worsens lesion size[42,44,45] or ameliorates injury[46]. This discrepancy may be in part explained by method of microglial depletion; pharmacologic approaches with CSF1R inhibitors can also impact peripheral microglia-like macrophages[47,48] and genetic approaches with diphtheria toxin A cause a peripheral inflammatory response[48,49] so may actually be stimulating peripheral macrophages. The role of sex in these studies is unclear; studies were completed only in male mice[44,45] or did not disaggregate data by sex.[46] One study[42] compared male and female mice and found microglial ablation aggravates injury only in males; the tamoxifen required to induce the genetic ablation of microglia may confound the reported sex differences.

The present study had two goals. First, we aimed to assess the impact of postnatal day 10 (P10) HI or a control procedure (Sham) on pathology, including lesion size and microglia density, on male and female mice. We report here a mild but clear sex-specific brain pathology after HI. Second, we aimed to determine if prior microglia depletion exacerbated or ameliorated a sex-specific impact of HI-induced pathology. Pharmacological depletion of microglia has traditionally been accomplished using CSF1R inhibitors, such as PLX3397, given orally over ~2 weeks.[50,51] Such slow depletion of microglia is untenable for perinatal HI studies where the injury is induced at P10 and the brain examined at P13, and where depletion close to P0 may disrupt development prior to the P10 injury. To address this challenge, we initiated a PLX3397 injection regimen at P7 that largely depletes brain microglia by P10 compared to vehicle-injected (Veh) mice. We then employ this novel PLX3397 regimen to assess if microglia depletion leads to sex-specific pathology outcomes in mice. Our data reveal a clear sex difference: in female HI mice, microglial depletion makes the pathology worse, while in male mice microglia depletion has a trend to decrease HI pathology. These data are discussed in light of the complex role of microglia in health and disease.

MATERIALS AND METHODS

Animals

Dams and males were C57BL/6J mice shipped from Jackson Laboratory and bred in the Children's Hospital of Philadelphia (CHOP) Research Institute. Dams were individually housed in a HEPA-filtered, closed airflow vivarium rack (Lab Products Inc., Enviro-Gard™ III) under a normal 12:12-hour light-dark cycle (06:00 on, 18:00 off) with *ad libitum* access to food (standard rodent chow, Lab Diets 5015 #0001328) and water. The AAALAC-accredited facility at the CHOP Research Institute is temperature- (22°C) and humidity-controlled (30-70%). Dams were housed with males for an average of 11 days before being singly-housed. Cages were checked for pups once daily in the late afternoon. Mouse pups were kept in the same cage as the dam and their littermates following birth and were not disturbed for 6 days.

Four cohorts of mice were included in this study. The first cohort received no drug treatment and only underwent HI or Sham at P10 for assessment of Iba1 response; this included 134 pups total across 18 litters with 73 males (25 Sham, 48 HI) and 61 females (20 Sham, 41 HI). The second cohort was used for a dose-response study for PLX3397 and included 18 pups total across 2 litters: 3 Veh (1 Female, 2 Male), 8 mice receiving 25mg/kg PLX3397 (4 Female, 4 Male), and 7 mice receiving 50mg/kg PLX3397 (3 Female, 4 Male). There was no mortality in the second cohort. The third cohort included one litter of 9 mice, 5 of which received 50mg/kg PLX3397 (2 Female-HI, 1 Female-Sham, 2 Male-HI) and 4 Veh mice (1 Female-HI, 1 Female-Sham, 2 Male-HI). Of these mice receiving 50mg/kg PLX mice, 80% were dead by P12 (100% of females including 2 HI and 1 Sham; 50% of HI males); there were no deaths in the Veh groups. The fourth cohort included the variables of drug (25mg/kg PLX3397 or Veh) and surgery (HI or Sham). This included 78 pups across 10 litters (40 males, 38 females; 10 Veh-Sham, 28 Veh-HI, 10 25mg/kg PLX3397-Sham, 30 25mg/kg PLX3397-HI). There was a 9% mortality rate (n=7) in the fourth cohort: 29% (n=2) of deaths were in the Male-25mg/kg PLX3397-HI group, 14% (n=1) were Female-25mg/kg PLX3397-HI, 29% (n=2) were Male-Veh-HI, 14% (n=1) were Female-Veh-HI, and 14% (n=1) were Female-Veh-Sham. There were no deaths in the Male-Veh-Sham group. Pups were weighed daily from P7 to P13.

All mice were cared for in compliance with protocols approved by the Institutional Animal Care and Use Committee at CHOP and guidelines established by the NIH's *Guide for the Care and Use of Laboratory Animals.* Our scientific reporting adheres to the ARRIVE 2.0 guidelines.[52]

PLX3397 injections

PLX3397 (PLX, Selleck, Catalog No.S7818) was resuspended in dimethyl sulfoxide (Cell Signaling Technology, Catalog No.12611P) to make a 50mM stock, which was frozen and stored (-80°C) in aliquots of 50μL. At P7, male and female littermates were randomly divided into groups. Mice received daily ~9AM intraperitoneal injections (*ip*) of 20μL PLX or injections of the same volume 20μL Vehicle (50% phosphate-buffered saline PBS, 50% polyethylene glycol). To perform a dose-response assessment (PLX given P7-P9, examined on P10), 19 pups from two litters were randomly assigned to three experimental groups: 50 mg/kg PLX, 25 mg/kg PLX, and Veh. Mice received daily ip injections from P7 to P9. Brains were collected at P10, 24 hours after the last PLX or Veh injection. For the rest of the PLX studies (including studies with HI/Sham), 25 mg/kg or Veh was given *ip* P7-P12 and brains were collected on P13, 24 hours after their last 25 mg/kg PLX or Veh injection.

Behavioral Testing

Developmental milestones and behavior were tested on postnatal days 8, 9, 12, and 13 as previously published.[53] At P8 and P9, forelimb grasp (strength) was measured using a custom-made 3D-printed forelimb grasp apparatus (https://github.com/EischLab/DevelopmentalMilestonesBehavior). Pups were placed vertically 10 cm over the table surface and forepaws were allowed to grip a 0.80 mm diameter rod (straightened paper clip); the length of time the pup gripped the rod was recorded. At P12, exploration was assessed by placing each mouse in the center of a 13 cm diameter circle (drawn on white paper) and recording the time until the pup exited the circle (latency to exit circle) or 120 seconds elapsed.[53] At P13, appearance and gross behavioral observations of pups were noted when the dam was removed, first in the homecage for 5 minutes, and then in a novel environment with littermates for an additional 5 minutes.

Hypoxia-Ischemia and Seizure Scores

A modified Vannucci Model[2,54–56] of HI was used in male and female PLX and Veh mice at P10. Male and female pups were randomly assigned to HI or Sham groups, ensuring as equal distribution as possible among all experimental groups within each litter. Briefly, lidocaine ointment was placed on the pup's ventral neck, then under isoflurane anesthesia (3% v/v for induction and 1% v/v for maintenance), a midline ventral incision in the anterior neck was made. Pups either underwent double ligation of the right common carotid artery with a 5.0 silk suture, or a Sham surgery that included incision and isolation of the right carotid artery without ligation. The entire surgery lasted ~5-7 minutes. Post-surgery, the mice recovered for 60-80 minutes on a heating pad with their littermates; temperatures of each individual pup were closely monitored and maintained between 36.0-37.9°C. Recovery was followed by 45 minutes of hypoxia exposure where oxygen concentration was decreased to 8% with balanced nitrogen in a controlled chamber (BioSpherix Ltd., Parish, NY, USA). The Sham mice remained the same amount of time in normoxia conditions (21% FiO_2). During hypoxia as well as 10 min before and 10 min after, mice were assessed on a modified Racine scale for seizure activity. Briefly, every 5 minutes pups were assigned a score from 0 to 6 to reflect maximal seizure activity in that bin of time. Baseline behavior received a score of 0, behavioral arrest or immobility (1), head bobbing or rigid posture (2), unilateral limb clonus (3), bilateral limb clonus (4), exhibiting level 4 clonus for most of the 5 minutes or level 4 for at least 30 seconds (5), and severe seizure activity with running or jumping (6). A cumulative seizure score was generated for each pup (ranging from 0-84). Across all experimental litters, the total time pups spent away from their dam was on average 120 minutes. Within each litter, time away from the dam was calculated for HI pups and averaged; all Sham mice spent exactly this time away from the dam.

Brain Collection and Tissue Preparation

Mice were killed at P10 or P13 via rapid decapitation using sterilized, surgical scissors in compliance with NIH guidelines for euthanasia of rodent neonates. Brains were then placed in room temperature (RT) 4% paraformaldehyde (PFA) and fixed for 72 hours. Following two PFA changes (1/day), brains were cryoprotected via placement in 30% sucrose in 0.1 M phosphate-buffered saline (PBS) at 4°C. Forty µm coronal sections were collected on a freezing microtome (Leica SM 2000 R) and stored in 1xPBS with 0.01% sodium azide at 4°C until processing for histological assessment. A subset of mice from the first cohort were not fixed, as detailed in the next section.

Pale Surface Brain Lesion: Presence and Size

For the presence of a pale lesion on the surface of the brain, each extracted brain underwent gross visual examination. If present, these pale brain surface lesions were always on the right hemisphere (due to right carotid artery ligation). For lesion size, if a pale surface lesion was present, a flexible ruler was placed on the surface of the brain to measure (in 0.5mm increments) the lesion at its greatest extent rostro-caudally and

medio-laterally; calculated lesion area was the product of the length x width of the lesion. Additional qualitative assessment of the surface brain lesion came from the brains from a subset of mice from the first cohort (26 mice across 4 litters, including both Male and Female, HI and Sham). These were not fixed and instead were examined for whole brain gross pathology followed by TTC staining. Briefly, after examination for the presence of a pale lesion on the brain surface, brains were cut into 1 mm coronal brain sections via placement in a brain matrix. Sections were submerged in 2% 2,3,4-Triphenyltetrazolium chloride (TTC, VWR Catalog number EM1.08380.0100) in 1x PBS and incubated at 37°C for 15 minutes. Sections were rinsed in PBS then fixed in 4% PFA at 4°C for at least 2 hours prior to imaging.

Immunohistochemistry (IHC) for Iba1

IHC was performed as previously described[57,58] using an antibody against Iba1, which labels both brain-resident microglia and monocyte-derived microglia-like macrophages that infiltrate the brain from the peripheral blood. Briefly, 40 µm brain sections were mounted onto charged slides (Thermo Fisher Scientific, #12-550-15) and left to dry for 1-2 h prior to IHC. Sections underwent antigen retrieval (0.01 M citric acid, pH 6.0, 100°C, 15 min) followed by room temperature (RT) washes in 1xPBS; all subsequent steps also occurred at RT. Non-specific protein binding was blocked via incubation with 3% Normal Donkey Serum (NDS) and 0.3% TritonX-100 in 1xPBS for 60 minutes. Following pretreatment and blocking steps, sections were incubated overnight with rabbit-anti-Iba1 (1:5000; Wako Chemicals, #019-19741) in a carrier of 3% NDS and 0.3% Tween-20 in 1xPBS. Approximately eighteen hours later, sections were rinsed with 1xPBS prior to incubation with biotinylated donkey-anti-rabbit IgG (1:200; Jackson ImmunoResearch Laboratories, #711-065-152) in a carrier of 1.5% NDS in 1xPBS. After washing with 1xPBS, endogenous peroxidase activity was inhibited via incubation with 0.3% hydrogen peroxide in 1xPBS for 30 min. Following an additional set of 1xPBS washes, slides were incubated with an avidin-biotin complex (ABC Elite, Vector Laboratories, #PK-6100) for 90 min. Slides were washed with 1xPBS and immunoreactive cells were visualized via incubation with metal-enhanced diaminobenzidine (Thermo Fisher Scientific, #34065) for 11-12 min. Slides were counterstained with Fast Red (Vector Laboratories, #H3403), dehydrated in a series of increasing ethanol concentrations and Citrosolv, and coverslipped with DPX (Thermo Fisher Scientific, #50-980-370).

Quantification of Iba1-immunoreactive (+) cells

Images from Iba1-immunostained sections were captured in bright-field light microscopy using an Olympus BX51 microscope with a 10x/0.3NA objective and an Olympus DP74 camera (widescreen aspect ratio, 16:10). For mice treated with HI or Sham but without PLX or Veh treatment (Fig. 1), Four images of the hippocampus per brain were obtained at -1.70, -2.30, -2.92mm relative to bregma, with two images at -2.92mm to capture the entire hippocampus at that bregma. Images were analyzed in Fiji by converting to RGB stack, then applying mask/threshold to blue image, which best captured DAB-labeling. Fiji reported for each image the percentage of pixels positive for Iba1 immunoreactivity. To quantify Iba1+ cell depletion after PLX-treatment, we manually counted Iba1+ cells in representative images rather than using Fiji. For each mouse in the pilot dose finding cohort, a total of five 100x left hemisphere sections from the striatum, cortex, and anterior, middle, and posterior hippocampus were examined (+0.97, -1.55, -1.91, -2.45, and -2.91mm from bregma). Guidelines for taking photomicrographic images were established to enable anatomical matching of subregions across hemispheres and mice and to reduce variation in taking photomicrographs. These guidelines were as follows: Striatum: the forceps minor of the corpus callosum was positioned in the top and lateral corner of the image. Cortex: the edge of the cingulum and corpus callosum were positioned at the bottom of the photomicrograph. Hippocampus: the dentate gyrus (DG) crest was placed in the lateral central screen such that the Hilus extended into the middle of the image. After photomicrographs were collected, using Fiji, a blinded observer, measured the area of the striatum, cortex, and hippocampus; and created a small square (400x400 pixels) in

which Iba1+ cells were manually counted. The area of the brain region was converted to mm^2 based on 1pixel=9.19 $x10^{-7}$ mm^2. The number of Iba1+ cells in the square was divided by the area of the brain region (in mm^2) to generate the 1ba1+ cell density of the particular brain region. Iba1+ cell density was measured for each brain region (striatum, cortex, hippocampus) present in each photomicrograph. Iba1+ cell densities were averaged such that each mouse was represented by one density value. *Iba1+ cell density determination via sampling for PLX-HI brains P13*. For each mouse, sections from three distances from bregma (+1.21mm, -2.27mm, and -3.63mm) underwent IHC for Iba1. From each section, a total of three 100x images were collected each encompassing the entire field with brain tissue, from the left dorsal (includes cortex and striatum in +1.21 from bregma; cortex and hippocampus in -2.27 and -3.63 from bregma), left ventral (includes cortex, striatum, and anterior commissure in +1.21 from bregma; cortex, amygdala, and lateral hypothalamus in -2.27 from bregma; cortex and hippocampus in -3.63 from bregma), and a midline field (includes striatum in +1.21 from bregma, thalamus in -2.27 from bregma, and mesencephalic reticular formation in-3.63 from bregma). Photomicrographs were collected by a person unaware of sex and treatment. In total, 9 images at 100x magnification were collected for each PLX-treated mouse. For PLX-treated mice, each image was manually reviewed and the number of Iba1+ cells per 100x field was counted; numbers ranged from 0 - 113 per image across all mice and all distances from bregma. The total number of Iba1+ cells per image was averaged across the 9 images for a single average value of Iba1+ cells per 100x field per mouse.

Cresyl Violet Staining and Lesion Scoring

Forty µm brains sections in a 1:12 sampling ratio ranging from bregma +1.41 to bregma -3.63 were mounted onto charged slides (Thermo Fisher Scientific, #12-550-15) and left to dry for 36 hours prior to staining with 0.1% cresyl violet acetate (CV). Lesion scoring for every section (range 7-11 sections per brain) was performed by two independent observers masked to experimental conditions in four hippocampal subregions (CA1, CA2, CA3, dentate gyrus), striatum, and cortex of all sections. The CA1 was defined as the most dorsal hippocampal subfield, formed by smaller, more dense pyramidal cell bodies than those observed in the CA2 and CA3. The CA2 was distinguished from the CA1 and CA3 by a widening of the pyramidal cell layer.[59] Striatum was scored between bregma +1.41mm to -1.2mm because striatum was not present in sections posterior to this bregma. The cortex was scored in all sections from +1.41mm to -3.63mm. The left and right hemispheres were each scored independently. The entirety of each region within a section was visually analyzed at 100x and 200x magnification and scored on a scale of 0-3 with the following criteria: 0 = no injury, 1 = scattered shrunken neurons, 2 = moderate cell loss with infarction in columnar distribution, 3 = severe cell loss with cystic infarction.[60] For each brain section, a score of 0-3 was given to each brain region analyzed. For each brain within each subregion, scores across bregma were averaged to yield average sub-region lesion scores. Average sub-region lesion scores from the two independent masked observers were averaged together to yield the final score graphed and analyzed; the average difference in lesion scores between observers was 1.6%. One observer scored all contralateral hemisphere sections; all scores were zero so the second observer scored only the ipsilateral hemisphere.

Statistical Analysis

Values are presented as mean ±standard deviation. All mice were included in all statistical analysis; there were no exclusions. Statistical analysis was performed using GraphPad Prism version 10.0.0 (GraphPad Software, Boston, Massachusetts USA). Analyses used and complete statistical outcomes are indicated in each figure legend for each figure panel or in the text when there is not a relevant figure. Statistical significance was defined at $p<0.05$. Effect size was determined via Cohen's d where small ($d \geq 0.2$), medium ($d \geq 0.5$), and large ($d \geq 0.8$) are based on previously defined benchmarks[61,62].

RESULTS

HI induced a pale brain surface lesion in a portion of mice, with a larger surface lesion in Male vs Female mice.

Mice underwent Sham or HI at P10 and brains were removed at P13 **(Fig. 1A)**. In all cohorts, whole brains were first examined for gross pathology, such as a pale lesion evident on the surface of the brain (**Supplemental [Supp.] Fig. 1**). No Sham mice had a pale lesion on the brain surface, as expected (Sham n = 45 in cohort 1, see 'Animals' section in Methods). However, of all 89 HI mice in cohort 1, 21% (19/89) had a detectable pale brain surface lesion. When considered by sex, 25% of the Male-HI mice (12/48) and 17% of the Female-HI mice (7/41) had a pale surface brain lesion. There was no significant correlation between sex and the presence of a pale lesion (Fisher's exact test, $p>0.05$). However, of the mice who did have a pale surface lesion, the lesion was ~2-fold larger in Male-HI mice compared with Female-HI mice, and there was more variance of lesion size in Male-HI compared with Female-HI mice **(Supp. Fig. 1)**. After gross examination, a subset of brains (26 mice across 4 litters, including HI and Sham, Male and Female) were then sectioned (1 mm slices) and processed for TTC. Qualitative assessment supported the presence of pale lesions only in HI mice **(Supp. Fig. 1)**. These data show that in the more severely impacted mice that show a pale lesion on the brain surface, HI-induced lesion size is larger in Male vs Female mice.

Iba1+ pixels are more prevalent in the hippocampus of Male-HI and Female-HI mice vs Male-Sham and Female-Sham mice, and with greater variation in Male-HI vs. Female-HI mice

Iba1 is a protein expressed in the brain by both microglia and infiltrating microglia-like macrophages, and increased number or density of Iba1+ cells is often seen after HI.[63–65] To assess Iba1 after HI and potential sex-dependent HI effects on Iba1, P13 brains were examined for Iba1+ cells after P10 HI or Sham **(Fig. 1A)**. Qualitative assessment of P13 brains revealed Iba1+ cells evident in the hippocampi of all Sham and HI mice **(Fig. 1B-E)**. In Sham mouse brains, Iba1+ cells were relatively evenly-spaced within recognizable brain regions and hippocampal subregions **(Fig. 1B, D)**. There was no qualitative difference in Iba1+ hippocampal cells in Male-Sham vs Female-Sham mice at P13, in keeping with prior work from P10 mice.[66] In contrast in HI mouse brains, Iba1+ cells were irregularly-spaced, with dark patches of cells or tissue appearing in an unpredictable pattern **(Fig. 1C, E)**. Quantitative assessment of the proportion of Iba1+ pixels in all four groups of mice revealed Female-HI mice had 194% more vs Female-Sham mice, and Male-HI mice had 261% more than Male-Sham mice **(Fig. 1F)**. There were also HI- and sex-dependent differences in variance. HI values varied more than Sham values within each sex. While Male-Sham and Female-Sham values had similar variance, Male-HI values varied more than Female-HI values **(Fig. 1F)**. These data underscore that HI at P10 increases Iba1 in the hippocampus at P13 relative to Sham, and that there is a sex-dependent difference in this HI impact: there is greater variance in Iba1+ pixels in Male-HI vs Female-HI mice.

25 mg/kg of the CSF1R inhibitor PLX3397 effectively depletes Iba1+ cells by P10 without disrupting weight or general developmental milestones

Most prior work with PLX3397 has given it orally for two weeks or longer[47,50], a duration which is not practical for testing the role of microglia in P10 HI injury. Therefore, we tested if injections of PLX3397 — either 25 or 50 mg/kg — given to mice starting at P7 would deplete brain Iba1+ cells by P10 **(Fig. 2A)**, the time when HI or Sham would be given to future cohorts. In regard to body weight, all three groups (Veh, 25 mg/kg PLX, 50 mg/kg PLX) were heavier on P10 than P7, showing they all gained weight over time. However, there were weight differences among the groups at two timepoints (P7, 50 mg/kg < 25 mg/kg and P10, 50 mg/kg < Veh**;** **Supp. Fig. 2**). In regard to Iba1+ cells, both 25 and 50 mg/kg PLX decreased Iba1+ cells throughout the brain relative to Veh injections. Qualitatively, even fewer Iba1+ cells were seen in 50 mg/kg PLX vs 25 mg/kg PLX

mice **(Fig. 2)**. However, a pilot study showed the 50 mg/kg dose of PLX led to unexpected mortality when combined with HI at P10 (data not shown). Based on this and based on 50 mg/kg mice weighing less than 25 mg/kg or Veh mice at P7 and P10, all subsequent cohorts received 25 mg/kg PLX or Veh. Quantification of the density of Iba1+ cells showed 97% fewer cells in 25 mg/kg PLX mice vs Veh mice **(Fig. 2)**. These data show that daily injections of 25 mg/kg PLX from P7 to P9 robustly eliminate Iba1+ cells when examined at P10, the time point when we planned to perform our HI.

Behavioral assessment of strength, exploration, and weight are not influenced by PLX, and HI does not influence exploration or weight.

Having established that 25 mg/kg PLX depletes microglia by P10, we next tested if continuous microglia depletion (injections P7-P12, brains collected 24 hr later on P13) would alter behavior or weight. We also tested if giving HI or Sham to Veh or PLX mice would change behavior or weight after the surgery **(Fig. 3A)**. In the forelimb grasp test, which looks at strength, all groups grasped for longer at P9 than at P8 with no additional differences **(Fig. 3B)**. In open field traversal at P12, a test of exploratory behavior, all groups had similar latencies to exit the circle **(Fig. 3C)**. Weights and fur state were also examined from P7 to P13, with negligible impact on weight **(Supp. Fig. 3)**. Analysis of only the final weight at P13 showed an interaction of Sex and HI/Sham treatment, but no post hoc differences among any groups **(Fig. 3D).** Fur state qualitatively changed in PLX mice over time **(Supp. Fig. 4)**. At P10 during surgery (not shown) and also at P13 **(Supp. Fig. 4A)**, PLX mice had a pinker ventrums vs. Veh mice. At P13, PLX mice also had notable hair on their snout, behind their ears, and along their fore- and hind paws vs. Veh mice **(Supp. Fig. 4B)**. These data show that PLX does not influence grasping, exploratory behavior, or weight, and that HI does not influence exploratory behavior or weight.

PLX did not influence HI-induced P10 seizure score or grossly impact the proportion of mice that show HI-induced pale brain surface lesion

Although PLX did not influence behavior or weight between P7 and P13, it is reasonable to ask if PLX given P7-P10 prior to HI or Sham surgery influenced an immediate effect of HI: seizure activity seen before, during, or after hypoxia. To this end, on P10, mice were observed prior to, during, and for 10 min post-hypoxia for evidence of seizure activity. The average total seizure scores during hypoxia were not different among the four groups (Multiple linear regression, Female-Veh-HI=26.92; Male-Veh-HI=27.83; Female-PLX-HI=28.46; Male-PLX-HI=23.83; Sex, $F(1,46)=1.076$, $p=0.305$; PLX/Veh, $F(1,46)=0.814$, $p=0.372$; interaction, $F(1, 46)=2.494$, $p=0.121$). Therefore, there was no effect of PLX (thus far given P7-P10) on HI-induced seizure activity.

While PLX did not influence this short-term effect of HI (P10 seizure activity), it is possible that PLX given P7-P12 changed a longer-term effect of HI: the proportion of HI mice that have a pale lesion on the surface of the extracted brain when examined on P13. As expected, no Sham mice (either PLX or Veh) of either sex had a pale lesion on the brain surface, in keeping with our earlier results **(Supp. Fig. 1)**. Of the 52 HI mice who received PLX or Veh injections, 12% (6/52) had a pale lesion on the surface of the brain. These six mice represented 0% of Female-Veh-HI (0/12), 21% of Female-PLX-HI (3/14), 15% of Male-Veh-HI (2/13), and 8% of Male-PLX-HI (1/13) mice. When visualized, these values appeared to suggest a sex-specific PLX effect; a greater proportion of Female-PLX-HI mice had a pale lesion vs. Female-Veh-HI mice, and a slightly lower proportion of Male-PLX-HI mice had a pale lesion vs. Male-Veh-HI mice **(Supp. Fig. 5)**. However, analysis showed no difference in the effect of PLX or Veh in Male or Female mice **(Supp. Fig. 5)**.

Iba1+ cell depletion worsens HI lesion scores in females but not males

As only a portion of HI mice of both sexes showed a pale lesion on the surface of the brain, we next utilized a more robust approach to assess HI-induced damage and the potential impact of sex and PLX: assigning a lesion score to thin cresyl-violet stained brain sections.[60] Therefore, brain regions (including the cortex, hippocampus, and hippocampal subregions) from most mice were assigned a lesion score ranging from 0 (no injury) to 3 (severe cell loss with cystic infarction; **Fig. 4A-T**). Both hemispheres were examined. However, stained sections from the contralateral hemisphere of every mouse — regardless of sex, treatment, or surgery condition — yielded lesion scores of zero. In addition, the ipsilateral hemispheres of all Sham mice yielded scores of zero. In the hippocampus **(Fig. 4U)**, Female-PLX-HI mice have a higher hippocampal lesion score vs Female-Veh-HI mice and Male-PLX-HI mice. In the hippocampus of males, Male-PLX-HI mice had a visually lower lesion score vs Male-Veh-HI mice, which was notably in the opposite direction from females; however, these visual effects were not statistically different. In the cortex **(Fig. 4V)**, there was statistical difference among the four groups, but the effect size between Female-PLX-HI and Female-Veh-HI was large (Cohen's d = 1.01) while the effect size between the Males was negligible (Cohen's d = -0.0337). Another way to visualize these lesion scores across the four groups in the hippocampus and cortex supports the impression that PLX increases lesion scores in Females and decreases lesion score in Males **(Fig. 4W, X)**. In hippocampal subregions **(Fig. 4Y-BB)**, lesion score analysis also suggested that PLX had an opposite effect in Female-HI and Male-HI mice. For example, in CA1 **(Fig. 4Y)**, Female-PLX-HI mice had a lower average lesion score vs Male-Veh-HI mice and Female-PLX-HI mice, with the effect size between the Male-PLX-HI and Male-Veh-HI groups was medium and negative (Cohen's d = -0.793), while the effect size between Female-PLX-HI and Female-Veh-HI mice was medium (Cohen's d = 0.642). In hippocampal CA2 **(Fig. 4Z)**, the effect size between the Female-PLX-HI and Female-Veh-HI was large (Cohen's d = 0.721) and the effect size between Male-PLX-HI and Male-Veh-HI mice was medium and negative (Cohen's d = -0.583). In hippocampal CA3 **(Fig. 4AA)**, Female-PLX-HI lesion scores were higher vs Female-Veh-HI and Male-PLX-HI, and the effect size between Female-PLX-HI and Female-Veh-HI was large (Cohen's d = 0.97) and the effect size between Male-PLX-HI and Male-Veh-HI was small and negative (Cohen's d = -0.388). The hippocampal DG was the only hippocampal subregion where PLX did not appear to influence lesion size **(Fig. 4BB)**, although no difference was seen in the striatum as well (data not shown). After determining lesion scores for each brain region, each HI mouse was then given an average ipsilateral lesion score, and this was compared to the seizure score (from P10) to assess any relationship. However, there was no correlation between the P10 seizure score and average ipsilateral lesion score **(Supp. Fig. 6)**. In sum, these data suggest that PLX injections from P7-P12 have opposite effects on P10 HI-induced lesions visualized at P13: PLX increases lesion scores in Female-HI mice, but PLX decreases lesion scores in Male-HI mice.

<u>PLX depletes Iba+ cells in Female and Male mice equally, and PLX-induced Iba1+ cell depletion does not correlate with HI-induced P10 seizure score</u>

One possible explanation for these disparate effects — PLX makes the lesion worse in Female-HI vs Female-Sham mice but has the opposite effect in Male mice — is that PLX depletes Iba1+ cells unequally in female vs male mice. To address this, Iba1+ brain sections from PLX and Veh mice were qualitatively and quantitatively assessed. Qualitatively, an observer blind to injection group could easily distinguish Iba1-stained sections from PLX **(Fig. 5A)** vs Veh mice **(Fig. 5B)**. There were far fewer Iba1+ cells in PLX mice, and the depletion after was dramatic and diffusely apparent throughout all brain regions visible (+1.21, -2.27, and -3.36mm relative to bregma). There was also a morphological difference in the few residual Iba1+ cells in PLX mice vs Iba+ cells in Veh mice. For example, in PLX mice Iba1+ cells were larger, thicker, and predominated in white matter tracts rather than gray matter areas. To assess a potential sex difference in PLX-induced Iba1+ cell depletion, we counted the low number of Iba1+ cells remaining in these PLX injected mice. Quantitatively, the low number of Iba1+ cells in PLX mice was similar in both sexes and in both HI and Sham mice (**Fig. 5C**).

Correlational analysis showed that the number of Iba1+ cells remaining in Female-PLX-HI and Male-PLX-HI mice did not correlate with the average ipsilateral lesion score (**Fig. 5D**). These findings suggest that the sex-dependent effect of PLX on HI-induced lesion score is not due to a sex-dependent effect of PLX on Iba1+ cell depletion.

DISCUSSION

In this study, we report two major findings. First, robust pharmacologic depletion of brain microglia by P10 is possible using daily *ip* injections of PLX3397 (P7-P9). Compared with giving this class of drugs orally over weeks, this method yields effective, rapid depletion that allows greater temporal precision to study the impact of microglia depletion in young animals. Second, PLX-induced depletion of Iba1+ cells prior to P10 HI leads to a worse HI lesion score in Female mice vs Veh Female mice, but not in Male mice; in fact, Male lesion scores appear to be improved by PLX vs Veh Males.

Our results are very interesting in the context of the literature. Two prior studies tested the effect of microglial depletion on HI-induced lesions and came to opposite conclusions. The first study, like us, used a pharmacological approach (PLX3397, 25 mg/kg) to deplete microglia and found smaller HI-induced lesions in microglia-depleted mice.[46] However, they used oral PLX administration and gave it to mice for 8 days (P4-P11, HI at P9) in contrast to our shorter 5-day *ip* administration of PLX (P7-P12, HI at P10). Also notable given our interest in sex-specific effects of microglia depletion is that this first study did not disaggregate their data by sex. The second study disaggregated their data by sex, and found that microglia depletion via inducible genetic modification (Cx3cr1$^{CreER/+}$Rosa26$^{DTA/+}$ mouse) increased the size of HI lesions in male — but not female — mice.[42] This is in contrast with our data, which show microglia depletion increased the HI-induced lesion in female — but not male — mice.

There are at least two explanations as to why our work shows microglia are protective in female (but not male) mice while this second study shows microglia are protective in male (but not female) mice. First, as the authors themselves note, the use of tamoxifen in their inducible genetic model may lead to a neuroprotective effect of this estrogen-like compound predominantly in female mice.[42] A second more comprehensive explanation for our conflicting results is that the respective approaches used to deplete microglia have different effects on peripheral microglia-like monocytes. More specifically, the genetic microglial depletion approach increases the number of peripheral Ly6C^{hi} monocytes, while the pharmacologic approach of PLX-induced depletion does not change this population.[47] Without microglial depletion, there may be underlying latent sex differences — when the same outcome is achieved through distinct mechanisms[67] — in the brain immune response to hypoxia-ischemia. We showed that both Males and Females increase Iba1+ cells 3 days after HI but that Males have more variability in the magnitude of their response (**Fig. 1**); these Iba1+ cells may be a combination of brain-resident microglia and monocyte-derived microglia-like cells (MGL cells) that infiltrate the brain after injury. If the Male Iba1+ cells have a greater proportion of MGL cells infiltrating from the periphery, and the genetic microglial depletion approach worsened peripheral inflammation, then it could be expected that lesion size worsens in Males after this experimental condition. If the Female Iba1+ cells after HI are predominantly brain resident microglia, then the Female response to injury may be less impacted by peripheral inflammation. Studies specifically detailing sex differences in relative contribution of microglia vs. MGL cells after HI will be useful, as well as evaluating if there are sex differences in how these MGL cells are called into the brain after injury. In general, this discrepancy of results highlights the importance of including both male and female mice and analyzing data separately in each sex, as the experimental manipulations may have opposite effects in each sex that could negate each other and create an illusion of no effect. Latent sex differences may not be revealed by HI alone, but may come to light after microglial depletion combined with HI.

Taken together, our findings are consistent with a hypothesis that after HI, brain-resident Female microglia act in a protective manner to mitigate brain injury, while the Iba1+ cells in Male brains may be comprised of more MGL cells infiltrating from the blood and worsening the injury. If this is true, then blocking MGL cells from entering the brain may prove to be an effective therapeutic target. This perspective warrants further investigation.

CONCLUSION

In this study, we established a model of pharmacologic depletion of Iba1+ cells in young mice. We find that depletion worsens HI-induced lesions in females but not in males. Our findings indicated that Iba1+ cells play a neuroprotective role in female mice after hypoxia-ischemia, but that this may be different in male mice.

List of abbreviations

HIE: Hypoxic Ischemic Encepalopathy
HI: Hypoxia Ischemia
PLX: 25mg/kg PLX3397
Veh: Vehicle
MGL: microglia-like
P: Postnatal Day

FIGURE LEGENDS

Figure 1. Early life hypoxia ischemia (HI) leads to more Iba1+ pixels in the hippocampus vs Sham mice, and more variance in the Iba1+ immunoreactivity in males than females. (A) Timeline: HI or Sham was induced at P10, and brains were collected at P13. Iba1-immunoreactive (+) cells were visualized, likely reflecting both brain-resident microglia and monocyte-derived microglia-like macrophages that infiltrate the brain from the peripheral blood. Subregions of the hippocampus indicated: CA1, CA2, CA3, dentate gyrus (DG). **(B-E)** Representative images of anterior hippocampal sections from a P13 Male-Sham mouse **(B)**, Male-HI mouse **(C),** Female-Sham mouse **(D)**, and Female-HI mouse **(E)**. **(F)** Percent of Iba1+ pixels in the hippocampus of P13 Sham and HI mice. Differences were seen within each sex, but not across sex. (Kruskal-Wallis, ***$p < 0.0001$. *Post hoc* Dunn's multiple comparisons: Female Sham vs Female HI, *$p = 0.020$; Male Sham vs Male HI, ***$p = 0.0001$; Female Sham vs Male Sham, $p > 0.999$; Female HI vs Male HI, $p > 0.999$). An F-test revealed more variance of Iba1+ pixels in Male HI vs Female HI mice ($F(22, 14) = 3.33$, $p = 0.006$), more variance in Female HI vs Female Sham ($F(14, 5) = 11.45$, $p <0.01$), and more variance in Male HI vs Male Sham ($F(22, 8) = 22.19$, $p <0.01$). Variance of Female Sham vs Male Sham was not different ($F(8, 5) = 1.72$, $p > 0.1$). Female Sham (n=6), Male Sham (n=9), Female HI (n=15), and Male HI (n=23). Magnification in **(B-E)** 100x; scale bar in **B**, 200µm.

Figure 2. PLX3397 (25 mg/kg) given from P7 to P9 almost completely depletes Iba1-immunoreactive (+) cells when examined on P10. (A) Timeline: Pups received a daily *ip* injection of Veh (2 male, 1 female), 25 mg/kg PLX (4 male, 4 female), or 50 mg/kg PLX (4 male, 3 female) from P7 to P9 and brains were collected 24 hours later on P10. Daily *ip* Veh or PLX injections are indicated by purple arrows. **(B-J)** Representative Iba1+ cell images of coronal sections from the hippocampus, cortex, and striatum in Veh, 25 mg/kg PLX, and 50 mg/kg PLX mice. Magnification 100x; scale bar **(B)** 200 µm, applies to **(B-J)**. For each mouse, five coronal sections that included the striatum, cortex, and anterior, middle, and posterior hippocampus (from bregma: 1.33, 0.97, -1.55, -2.45, and -2.91mm) were examined for Iba1+ cells counted in the left hemisphere. **(F)** Iba1+ cell density in 25 mg/kg PLX (median = 8.471, n = 8) mice was 97% less than Veh mice (median = 365.6, n = 3; Mann Whitney $U = 0$, * $p = 0.0121$).

Figure 3. PLX given from P7 to P13 does not change strength, exploration, or weight, and HI given at P10 does not change exploration or weight. (A) Timeline. Forelimb grasp (P8 and P9, pre-HI and pre-Sham surgery) and open field traversal (P12) were tested in HI and Sham mice. All behaviors were assessed 30-45 min after the daily *ip* injection (purple arrows) of PLX (25 mg/kg) or Veh. **(B)** The forelimb grasp, a test of strength, was performed on P8 and P9 mice, prior to HI or Sham surgery. Therefore, mice are grouped by sex (Female: orange bar outline/fill; Male: blue bar outline/fill) and injection (Veh: gray outlined circle icon; PLX: gray filled circle icon). P9 mice grasped for longer than at P8 (Mixed effect analysis, effect of Time, $F(1, 58)=25.37$, ***$p<0.0001$). There was no main effect of Sex or PLX/Veh $F(3,73)=1.235$, $p=0.303$, $p>0.05$) and no interaction of Time with Sex and PLX/Veh (Mixed effect analysis, $F(3,58)=1.144$, $p=0.339$, $p>0.05$). Female-Veh (n=17), Female-PLX (n=20), Male-Veh (n=20), and Male-PLX (n=20). **(C)** Open field traversal, a test of exploratory behavior, was performed on P12 two days after HI or Sham. All groups had similar times in P12 open-field traversal (latency to exit circle, 3-way ANOVA, Sex: ($F(1,63)=0.1877$, $p=0.666$), $p>0.05$; PLX: ($F(1,63)=1.088$, $p=0.301$), $p>0.05$; HI: ($F(1,63)=1.600$, $p=0.211$), $p>0.05$; interactions all $p>0.05$). **(D)** Body weights were assessed P7 to P13 **(Supp. Fig. 3)** with P13 data shown here separately. At P13, there was an interaction of Sex and HI/Sham ($F (1, 63) = 7.031$, *$p = 0.010$) and an effect of Sex ($F (1, 63) = 4.162$, *$p = 0.046$), but no effect of PLX ($F (1, 63) = 0.550$, $p = 0.461$) or HI/Sham ($F (1, 63) = 2.329$, $p = 0.132$) on weight. *Post hoc* analysis did not reveal any differences. Sample size for Open Field Traversal and weights at P13: Female-Veh-Sham (n=4), Female-PLX-Sham (n=5), Female-Veh-HI (n=12), Female-PLX-HI (n=14),

Male-Veh-Sham (n=4), Male-PLX-Sham (n=5), Male-Veh-HI (n=13), and Male-PLX-HI (n=13). F, Female. g, grams. HI, hypoxia-ischemia. M, Male. PLX, PLX3397. s, seconds.

Figure 4. PLX-mediated Iba1+ cell depletion worsens injury score in HI female mice but not in HI male mice. (A-T) Qualitative assessment of HI-induced lesions via cresyl violet-stained cortical and hippocampal sections. Brains were fixed and sectioned (40µm, coronal); sections analyzed were from +1.21 to -3.63 relative to bregma with a section sampling fraction of ⅙. Six brain regions (CA1, CA2, CA3, dentate gyrus, striatum, cortex) were given a whole number score between 0-3 with the following criteria: 0 = no injury, 1 = scattered shrunken neurons, 2 = moderate cell loss with infarction in columnar distribution, 3 = severe cell loss with cystic infarction. Arrowheads indicate shrunken neurons; arrows indicate columnar cell loss. **(A-D)**, **(I-L)** 100x magnification, scale bar = 200 µm. **(E-H)**, **(M-T)** 200x magnification, scale bar = 100 µm. **(U-BB)** Average lesion score for the **(U)** hippocampus, **(V)** cortex, **(Y)** CA1, **(Z)** CA2, **(AA)** CA3, and **(BB)** dentate gyrus and lesion severity for the **(W)** hippocampus and **(X)** cortex. **(U)** In the hippocampus (average of scores from CA1, CA2, CA3, and dentate gyrus for each subject), analysis of average lesions score revealed an interaction (2-way ANOVA, Interaction p=0.013), with *post hoc* analysis showing Female PLX-HI mice have a higher average lesion score vs Female Veh-HI mice and Male PLX-HI mice (Fisher's LSD, $p < 0.05$). The effect size between the Female PLX-HI and Female Veh-HI groups was large (Cohen's d = 0.873). There was no *post hoc* difference between the males, but there was visually a lower lesion score in Male PLX-HI v. Male Veh-HI (opposite direction from females), and the effect size for the males was medium (0.578). **(V)** In the cortex, analysis of average lesions score via ANOVA did not result in significant main effects or an interaction. However, the effect size between the Females was large (Cohen's d = 1.01) and the effect size between the Males was negligible (Cohen's d = -0.0337). **(W, X)** To visualize the differences between Veh and PLX groups in the hippocampus and cortex **(U-V)**, lesion scores in each group were binned in 0.5 increments and data were color-coded and plotted as the proportion of all mice in a group. **(Y)** In CA1, analysis of average lesions score revealed an interaction (2-way ANOVA, Interaction p=0.013), with *post hoc* analysis showing Male PLX-HI mice have a lower average lesion score vs Male Veh-HI mice and Female PLX-HI mice (Fisher's LSD, $p < 0.05$). The effect size between the Male PLX-HI and Male Veh-HI groups was medium and negative (Cohen's d = -0.793). The effect size between Females was medium (Cohen's d = 0.642). **(Z)** In CA2, analysis of average lesion score revealed an interaction (2-way ANOVA, Interaction p = 0.023) but no *post hoc* differences. The effect size between the Females was large (Cohen's d = 0.721) and the effect size between the Males was medium and negative (Cohen's d = -0.583). **(AA)** In CA3, analysis of average lesion score revealed an interaction (2-way ANOVA, Interaction p = 0.019) with *post hoc* analysis revealing higher scores in Female PLX-HI v. Female Veh-HI and Male PLX-HI (Fisher LSD *post hoc* $p < 0.05$). The effect size between the Females was large (Cohen's d = 0.97) and the effect size between the Males was small and negative (Cohen's d = -0.388). **(BB)** In DG, analysis of average lesions score via ANOVA did not result in significant main effects or an interaction. The effect size between the Females was large and negative (Cohen's d = -1.17). Sample size: Female, Veh-HI (n=12); Female, 25 mg/kg PLX3397-HI (n=14); Male, Veh-HI (n=13); and Male, 25 mg/kg PLX3397-HI (n=13).

Figure 5. PLX-induced depletion of Iba1+ cells is equivalent in Male and Female mice and does not correlate with lesion score. **(A-B)** Representative photomicrographs of the cerebral cortex (+1.21mm from bregma) in the brains of mice that received PLX (**A**; 25 mg/kg *ip*, daily P7-P12) or Veh (**B**) and underwent immunohistochemistry for Iba1. 100x magnification, scale bar **(A)** = 200 µm, applies **(A-B).** Note the lack of brown Iba1+ cells in the PLX mouse **(A)** compared to the Veh mouse **(B)**. **(C)** Quantitative assessment of Iba1+ cells. In each PLX mouse, 9 different 100x imaging fields were obtained (3 images at each of 3 different bregma). The total number of Iba1+ cells per image was manually counted then averaged across 9 images; this yielded an average value of Iba1+ cells per 100x field per mouse. There was no difference in Iba1+ cell

number among the four groups (2-way ANOVA; Male vs Female, $F(1, 33)=0.123$, $p=0.728$; HI vs Sham, $F(1, 33)=0.005$", $p=0.945$; Interaction $F(1, 33)=0.270$, $p = 0.607$). **(D)** Correlational analysis of average ipsilateral lesion score and Iba1+ cell loss. Among Female-PLX-HI mice ($R^2 = 0.070$, $F(1,12)=0.747$, $p=0.404$, n=14) and Male-PLX-HI mice ($R^2 = 0.050$, $F(1,11)=0.577$, $p=0.463$, n=13), Iba1+ cell number did not correlate with the average ipsilateral lesion score (average of all subregion scores). Subject number **(C, D)**: Female-PLX-Sham n=5, Female-PLX-HI n=14, Male-PLX-Sham n=5, Male-PLX-HI n=13

FIGURES

Figure 1

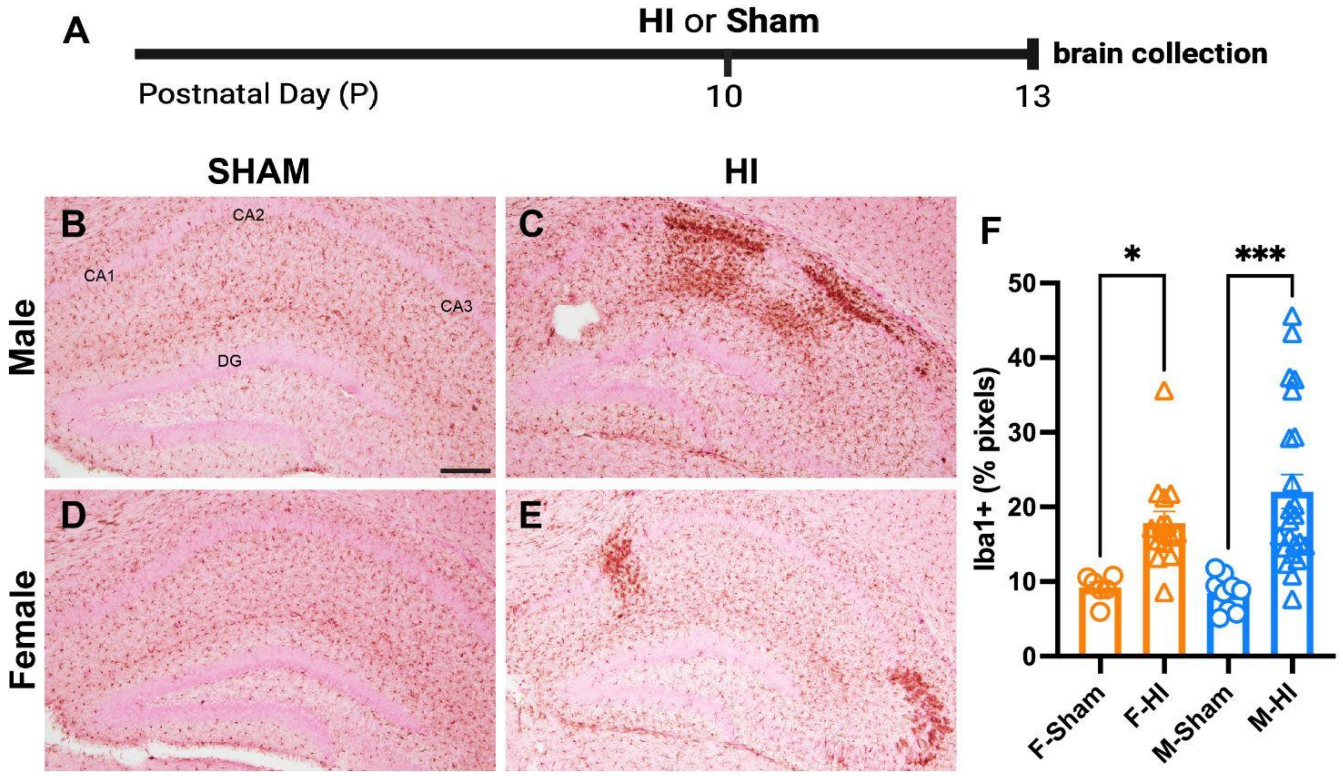

Figure 2

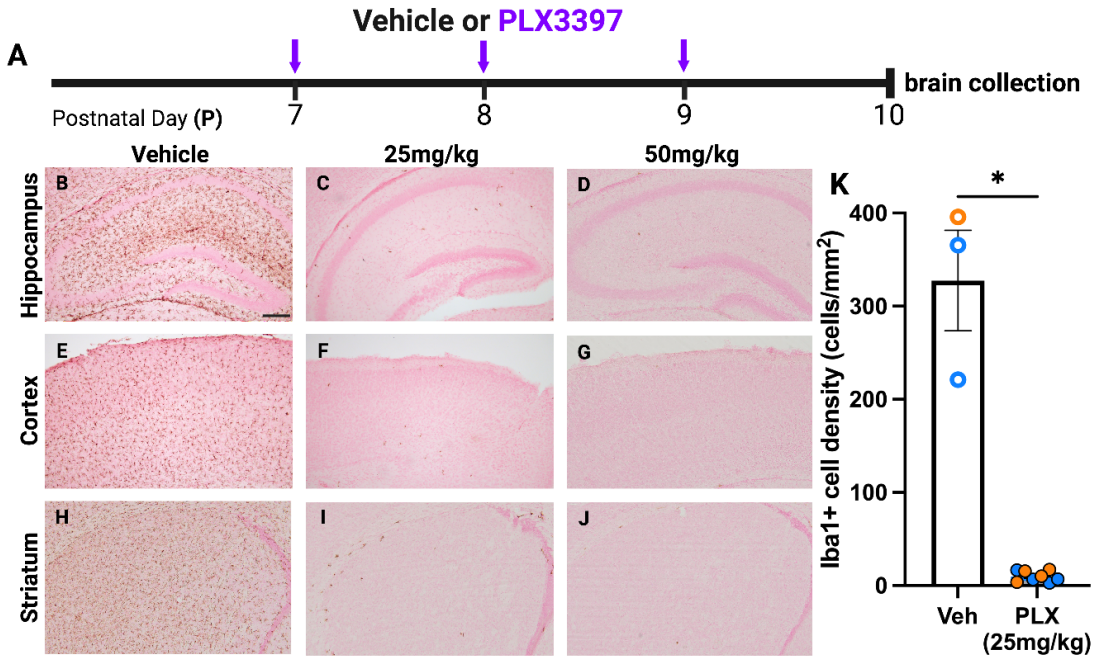
A
Vehicle or PLX3397
brain collection
Postnatal Day (P)
7
8
9
10
Vehicle
25mg/kg
50mg/kg
Hippocampus
Cortex
Striatum
B
C
D
E
F
G
H
I
J
K
*
Iba1+ cell density (cells/mm2)
400
300
200
100
0
Veh
PLX
(25mg/kg)

Figure 3

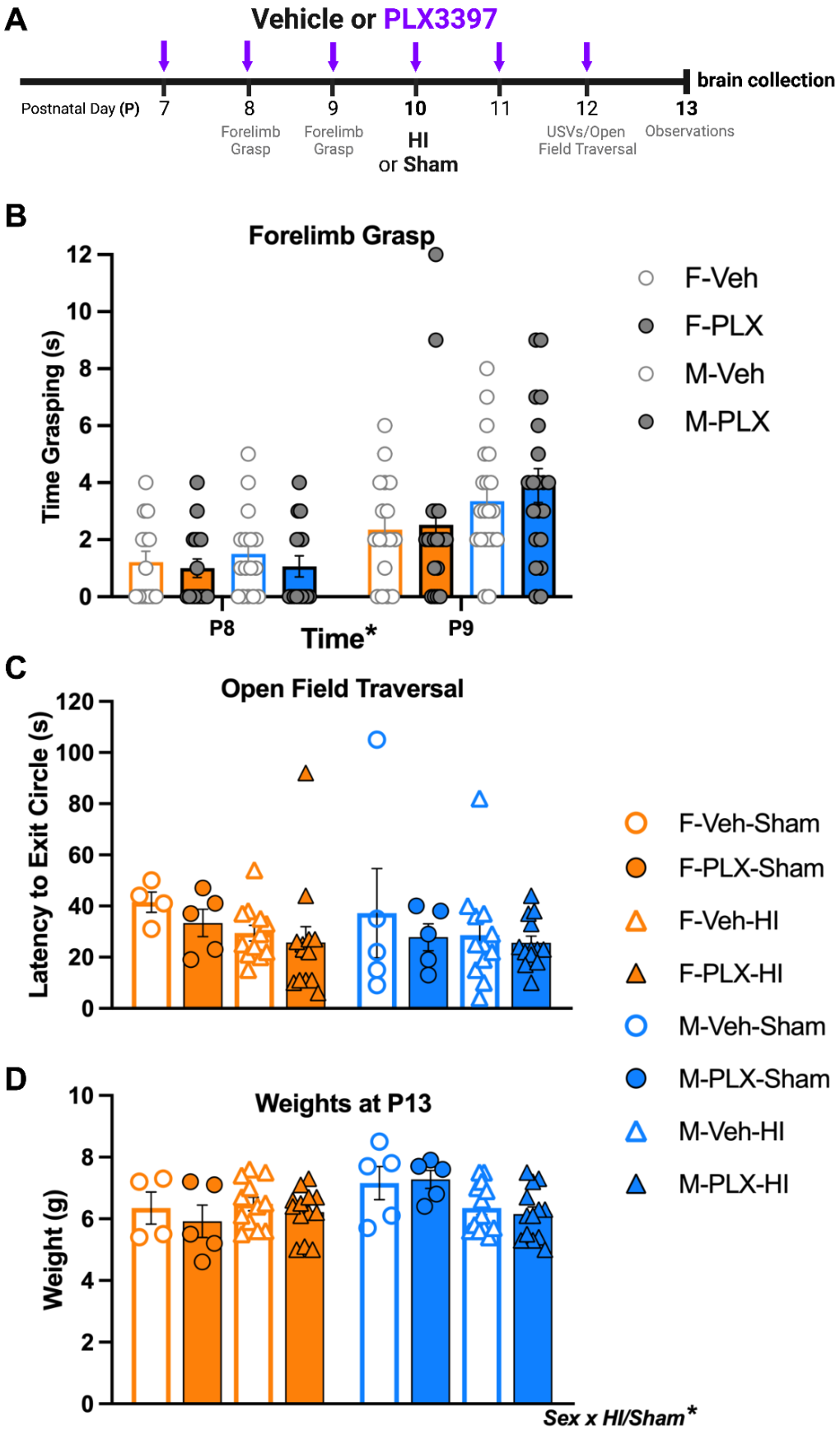
A
Vehicle or PLX3397
brain collection
Postnatal Day (P)
7
8
9
10
11
12
13
Forelimb Grasp
Forelimb Grasp
HI or Sham
USVs/Open Field Traversal
Observations
B
Forelimb Grasp
Time Grasping (s)
P8
Time*
P9
F-Veh
F-PLX
M-Veh
M-PLX
C
Open Field Traversal
Latency to Exit Circle (s)
F-Veh-Sham
F-PLX-Sham
F-Veh-HI
F-PLX-HI
M-Veh-Sham
M-PLX-Sham
M-Veh-HI
M-PLX-HI
D
Weights at P13
Weight (g)
Sex x HI/Sham*

Figure 4

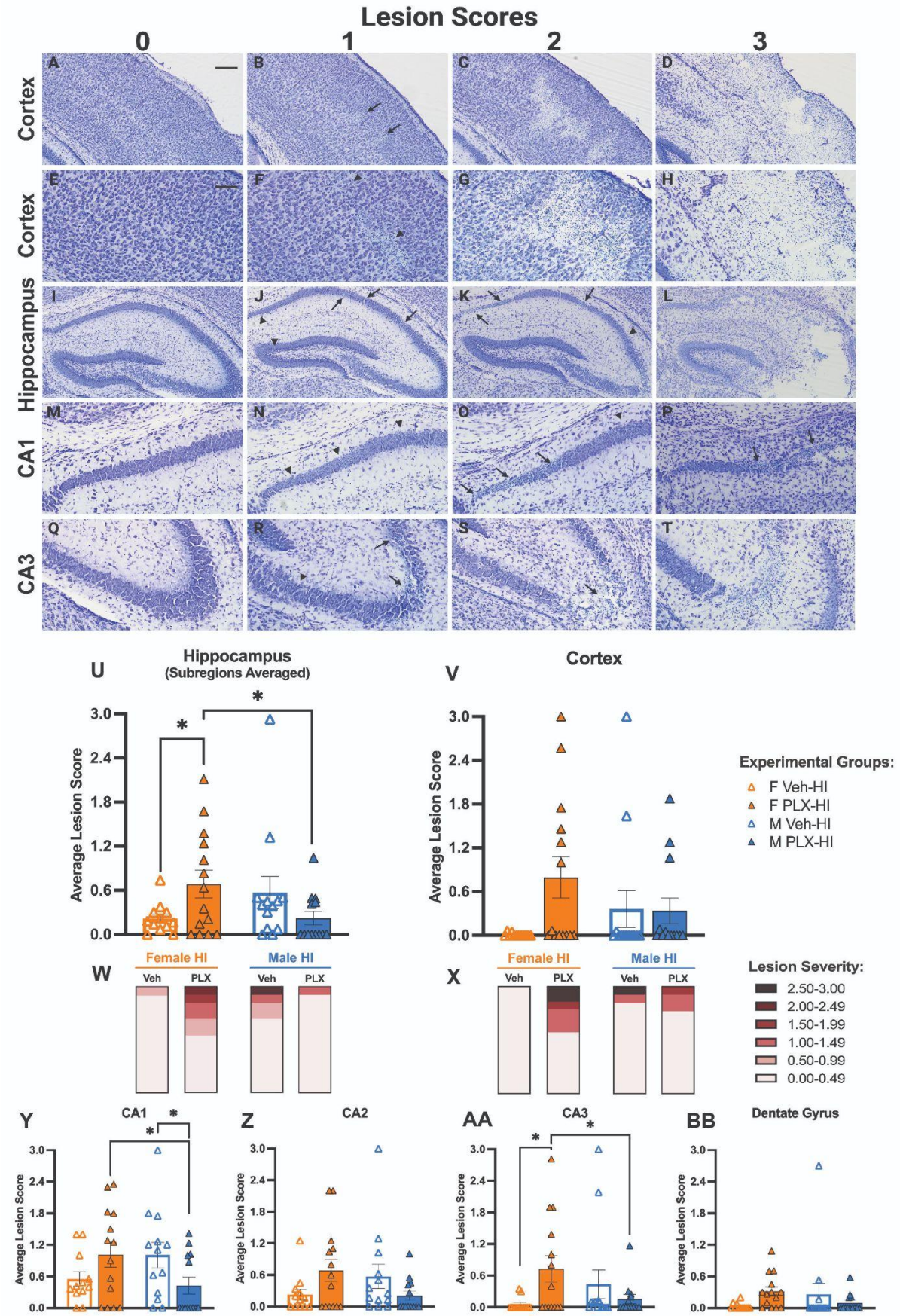
Lesion Scores
0
1
2
3
Cortex
Cortex
Hippocampus
CA1
CA3
A
B
C
D
E
F
G
H
I
J
K
L
M
N
O
P
Q
R
S
T
U
Hippocampus
(Subregions Averaged)
V
Cortex
Average Lesion Score
Experimental Groups:
F Veh-HI
F PLX-HI
M Veh-HI
M PLX-HI
W
X
Female HI
Male HI
Veh
PLX
Lesion Severity:
2.50-3.00
2.00-2.49
1.50-1.99
1.00-1.49
0.50-0.99
0.00-0.49
Y
CA1
Z
CA2
AA
CA3
BB
Dentate Gyrus

Figure 5

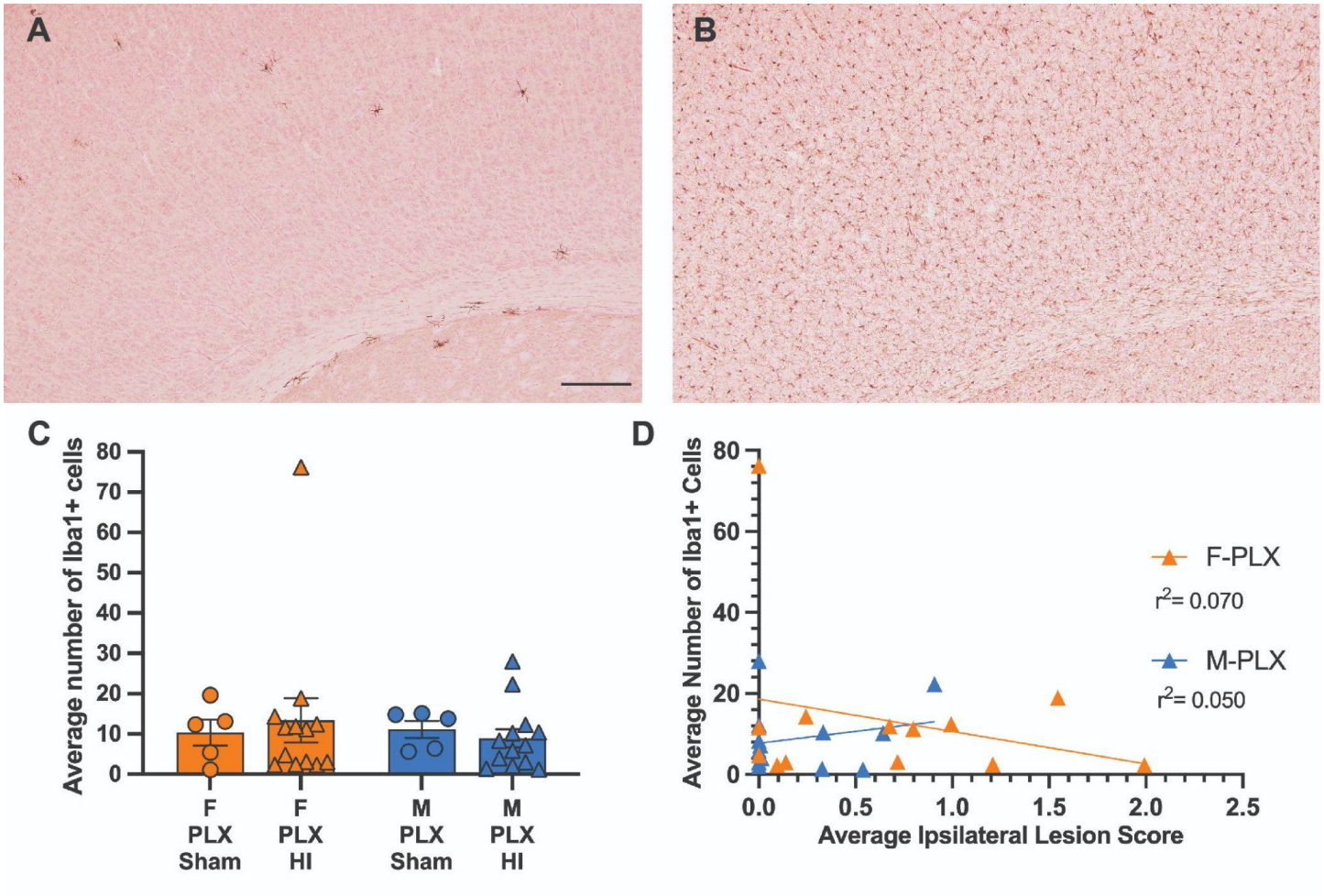
A
B
C
Average number of Iba1+ cells
80
70
60
50
40
30
20
10
0
F PLX Sham
F PLX HI
M PLX Sham
M PLX HI
D
Average Number of Iba1+ Cells
80
60
40
20
0
0.0
0.5
1.0
1.5
2.0
2.5
Average Ipsilateral Lesion Score
F-PLX
r2= 0.070
M-PLX
r2= 0.050

REFERENCES

1. Ferriero, D. M. Neonatal Brain Injury. *N. Engl. J. Med.* **351,** 1985–1995 (2004).
2. Millar, L. J., Shi, L., Hoerder-Suabedissen, A. & Molnár, Z. Neonatal Hypoxia Ischaemia: Mechanisms, Models, and Therapeutic Challenges. *Front. Cell. Neurosci.* **11,** 78 (2017).
3. Institute for Health Metrics and Evaluation (IHME). Causes of Death (COD) Data Visualization. Seattle, WA: IHME, University of Washington, 2018. at <http://vizhub.healthdata.org/cod>
4. Jennifer C. Burnsed, Raul Chavez-Valdez, Mir Shanaz Hossain, Kalpashri Kesavan, Lee J. Martin, Jiangyang Zhang, Frances J. Northington. Hypoxia-Ischemia and TherapeuticHypothermia in the Neonatal Mouse Brain–A Longitudinal Study. *PLoS One* (2015). doi:10.1371/journal.pone.0118889
5. Mirza, M. A., Ritzel, R., Xu, Y., McCullough, L. D. & Liu, F. Sexually dimorphic outcomes and inflammatory responses in hypoxic-ischemic encephalopathy. *J. Neuroinflammation* **12,** 32 (2015).
6. van de Looij, Y., Chatagner, A., Hüppi, P. S., Gruetter, R. & Sizonenko, S. V. Longitudinal MR assessment of hypoxic ischemic injury in the immature rat brain. *Magn. Reson. Med.* **65,** 305–312 (2011).
7. Smith, A. L., Alexander, M., Rosenkrantz, T. S., Sadek, M. L. & Fitch, R. H. Sex differences in behavioral outcome following neonatal hypoxia ischemia: insights from a clinical meta-analysis and a rodent model of induced hypoxic ischemic brain injury. *Exp. Neurol.* **254,** 54–67 (2014).
8. Diaz, J., Abiola, S., Kim, N., Avaritt, O., Flock, D., Yu, J., Northington, F. J. & Chavez-Valdez, R. Therapeutic Hypothermia Provides Variable Protection against Behavioral Deficits after Neonatal Hypoxia-Ischemia: A Potential Role for Brain-Derived Neurotrophic Factor. *Dev. Neurosci.* **39,** 257–272 (2017).
9. Aravamuthan, B. R., Gandham, S., Young, A. B. & Rutkove, S. B. Sex may influence motor phenotype in a novel rodent model of cerebral palsy. *Neurobiol. Dis.* **134,** 104711 (2020).
10. Wood, T. R., Gundersen, J. K., Falck, M., Maes, E., Osredkar, D., Løberg, E. M., Sabir, H., Walløe, L. & Thoresen, M. Variability and sex-dependence of hypothermic neuroprotection in a rat model of neonatal hypoxic-ischaemic brain injury: a single laboratory meta-analysis. *Sci. Rep.* **10,** 10833 (2020).
11. McCarthy, M. M. A new view of sexual differentiation of mammalian brain. *J. Comp. Physiol. A Neuroethol. Sens. Neural Behav. Physiol.* **206,** 369–378 (2020).
12. McCarthy, M. M. Sex and the Developing Brain Second Edition. *Colloquium Series on The Developing*

Brain **6,** i–141 Preprint at https://doi.org/10.4199/c00152ed1v01y201703dbr014 (2017)

13. Arnold, A. P. & McCarthy, M. M. in *Neuroscience in the 21st Century: From Basic to Clinical* (eds. Pfaff, D. W. & Volkow, N. D.) 2139–2168 (Springer New York, 2016).
14. Johnston, M. V. & Hagberg, H. Sex and the pathogenesis of cerebral palsy. *Dev Med Child Neurol* (2007). doi:10.1111/j.1469-8749.2007.0199a.x
15. Zhu, C., Xu, F., Wang, X., Shibata, M., Uchiyama, Y., Blomgren, K. & Hagberg, H. Different apoptotic mechanisms are activated in male and female brains after neonatal hypoxia-ischaemia. *J. Neurochem.* **96,** 1016–1027 (2006).
16. Hagberg, H., Wilson, M. A., Matsushita, H., Zhu, C., Lange, M., Gustavsson, M., Poitras, M. F., Dawson, T. M., Dawson, V. L., Northington, F. & Johnston, M. V. PARP-1 gene disruption in mice preferentially protects males from perinatal brain injury. *J. Neurochem.* **90,** 1068–1075 (2004).
17. Manole, M. D., Tehranian-DePasquale, R., Du, L., Bayir, H., Kochanek, P. M. & Clark, R. S. B. Unmasking sex-based disparity in neuronal metabolism. *Curr. Pharm. Des.* **17,** 3854–3860 (2011).
18. McCarthy, M. M. Sex differences in neuroimmunity as an inherent risk factor. *Neuropsychopharmacology* **44,** 38–44 (2019).
19. Gal-Oz, S. T., Maier, B., Yoshida, H., Seddu, K., Elbaz, N., Czysz, C., Zuk, O., Stranger, B. E., Ner-Gaon, H. & Shay, T. ImmGen report: sexual dimorphism in the immune system transcriptome. *Nat. Commun.* **10,** 4295 (2019).
20. McCarthy, M. M., Nugent, B. M. & Lenz, K. M. Neuroimmunology and neuroepigenetics in the establishment of sex differences in the brain. *Nat. Rev. Neurosci.* **18,** 471–484 (2017).
21. Smith, P. L. P., Mottahedin, A., Svedin, P., Mohn, C.-J., Hagberg, H., Ek, J. & Mallard, C. Peripheral myeloid cells contribute to brain injury in male neonatal mice. *J. Neuroinflammation* **15,** 301 (2018).
22. Chavez-Valdez, R., Mottahedin, A., Stridh, L., Yellowhair, T. R., Jantzie, L. L., Northington, F. J. & Mallard, C. Evidence for Sexual Dimorphism in the Response to TLR3 Activation in the Developing Neonatal Mouse Brain: A Pilot Study. *Front. Physiol.* **10,** 306 (2019).
23. Li, B., Concepcion, K., Meng, X. & Zhang, L. Brain-immune interactions in perinatal hypoxic-ischemic brain injury. *Prog. Neurobiol.* **159,** 50–68 (2017).
24. Villa, A., Gelosa, P., Castiglioni, L., Cimino, M., Rizzi, N., Pepe, G., Lolli, F., Marcello, E., Sironi, L., Vegeto,

E. & Maggi, A. Sex-Specific Features of Microglia from Adult Mice. *Cell Rep.* **23,** 3501–3511 (2018).

25. Sorge, R. E., Mapplebeck, J. C. S., Rosen, S., Beggs, S., Taves, S., Alexander, J. K., Martin, L. J., Austin, J.-S., Sotocinal, S. G., Chen, D., Yang, M., Shi, X. Q., Huang, H., Pillon, N. J., Bilan, P. J., Tu, Y., Klip, A., Ji, R.-R., Zhang, J., Salter, M. W. & Mogil, J. S. Different immune cells mediate mechanical pain hypersensitivity in male and female mice. *Nat. Neurosci.* **18,** 1081–1083 (2015).
26. Moriarty, O., Tu, Y., Sengar, A. S., Salter, M. W., Beggs, S. & Walker, S. M. Priming of adult incision response by early life injury: neonatal microglial inhibition has persistent but sexually dimorphic effects in adult rats. *J. Neurosci.* (2019). doi:10.1523/JNEUROSCI.1786-18.2019
27. Salter, M. W. & Stevens, B. Microglia emerge as central players in brain disease. *Nat. Med.* **23,** 1018–1027 (2017).
28. Bennett, M. L. & Bennett, F. C. The influence of environment and origin on brain resident macrophages and implications for therapy. *Nat. Neurosci.* **23,** 157–166 (2020).
29. Stevens, B., Allen, N. J., Vazquez, L. E., Howell, G. R., Christopherson, K. S., Nouri, N., Micheva, K. D., Mehalow, A. K., Huberman, A. D., Stafford, B., Sher, A., Litke, A. M., Lambris, J. D., Smith, S. J., John, S. W. M. & Barres, B. A. The classical complement cascade mediates CNS synapse elimination. *Cell* **131,** 1164–1178 (2007).
30. Schafer, D. P., Lehrman, E. K., Kautzman, A. G., Koyama, R., Mardinly, A. R., Yamasaki, R., Ransohoff, R. M., Greenberg, M. E., Barres, B. A. & Stevens, B. Microglia sculpt postnatal neural circuits in an activity and complement-dependent manner. *Neuron* **74,** 691–705 (2012).
31. Paolicelli, R. C., Bolasco, G., Pagani, F., Maggi, L., Scianni, M., Panzanelli, P., Giustetto, M., Ferreira, T. A., Guiducci, E., Dumas, L., Ragozzino, D. & Gross, C. T. Synaptic pruning by microglia is necessary for normal brain development. *Science* **333,** 1456–1458 (2011).
32. Zhang, J., Malik, A., Choi, H. B., Ko, R. W. Y., Dissing-Olesen, L. & MacVicar, B. A. Microglial CR3 activation triggers long-term synaptic depression in the hippocampus via NADPH oxidase. *Neuron* **82,** 195–207 (2014).
33. Bian C, Zhao ZQ, Zhang YQ, Lu N. Involvement of CX3CL1/CX3CR1 signaling in spinal long term potentiation. *PLoS One* **10,** e0118842 (2015).
34. VanRyzin, J. W., Marquardt, A. E., Argue, K. J., Vecchiarelli, H. A., Ashton, S. E., Arambula, S. E., Hill, M.

N. & McCarthy, M. M. Microglial Phagocytosis of Newborn Cells Is Induced by Endocannabinoids and Sculpts Sex Differences in Juvenile Rat Social Play. *Neuron* (2019). doi:10.1016/j.neuron.2019.02.006

35. Hellwig, S., Brioschi, S., Dieni, S., Frings, L., Masuch, A., Blank, T. & Biber, K. Altered microglia morphology and higher resilience to stress-induced depression-like behavior in CX3CR1-deficient mice. *Brain Behav. Immun.* **55,** 126–137 (2016).
36. Lenz, K. M., Nugent, B. M., Haliyur, R. & McCarthy, M. M. Microglia are essential to masculinization of brain and behavior. *J. Neurosci.* **33,** 2761–2772 (2013).
37. Guez-Barber, D., Wragan, M., Raphael, D., Phillips, H. M., Lu, K., Yun, S. & Eisch, A. J. Iba1+ cell density and morphology classification at postnatal day 10 in four hippocampal subregions of female and male C57BL/6J mice. doi:10.1101/2021.08.11.456021
38. Schwarz, J. M., Sholar, P. W. & Bilbo, S. D. Sex differences in microglial colonization of the developing rat brain. *J. Neurochem.* **120,** 948–963 (2012).
39. Nelson, L. H., Warden, S. & Lenz, K. M. Sex differences in microglial phagocytosis in the neonatal hippocampus. *Brain Behav. Immun.* **64,** 11–22 (2017).
40. Hanamsagar, R., Alter, M. D., Block, C. S., Sullivan, H., Bolton, J. L. & Bilbo, S. D. Generation of a microglial developmental index in mice and in humans reveals a sex difference in maturation and immune reactivity. *Glia* **66,** 1504–1520 (2018).
41. Thion, M. S., Low, D., Silvin, A., Chen, J., Grisel, P., Schulte-Schrepping, J., Blecher, R., Ulas, T., Squarzoni, P., Hoeffel, G., Coulpier, F., Siopi, E., David, F. S., Scholz, C., Shihui, F., Lum, J., Amoyo, A. A., Larbi, A., Poidinger, M., Buttgereit, A., Lledo, P.-M., Greter, M., Chan, J. K. Y., Amit, I., Beyer, M., Schultze, J. L., Schlitzer, A., Pettersson, S., Ginhoux, F. & Garel, S. Microbiome Influences Prenatal and Adult Microglia in a Sex-Specific Manner. *Cell* **172,** 500–516.e16 (2018).
42. Tsuji, S., Di Martino, E., Mukai, T., Tsuji, S., Murakami, T., Harris, R. A., Blomgren, K. & Åden, U. Aggravated brain injury after neonatal hypoxic ischemia in microglia-depleted mice. *J. Neuroinflammation* **17,** 111 (2020).
43. Pimentel-Coelho, P. M., Michaud, J.-P. & Rivest, S. Evidence for a gender-specific protective role of innate immune receptors in a model of perinatal brain injury. *J. Neurosci.* **33,** 11556–11572 (2013).
44. Szalay, G., Martinecz, B., Lénárt, N., Környei, Z., Orsolits, B., Judák, L., Császár, E., Fekete, R., West, B.

L., Katona, G., Rózsa, B. & Dénes, Á. Microglia protect against brain injury and their selective elimination dysregulates neuronal network activity after stroke. *Nat. Commun.* **7,** 11499 (2016).

45. Jin, W.-N., Shi, S. X.-Y., Li, Z., Li, M., Wood, K., Gonzales, R. J. & Liu, Q. Depletion of microglia exacerbates postischemic inflammation and brain injury. *J. Cereb. Blood Flow Metab.* **37,** 2224–2236 (2017).
46. Zhang, B., Ran, Y., Wu, S., Zhang, F., Huang, H., Zhu, C., Zhang, S. & Zhang, X. Inhibition of Colony Stimulating Factor 1 Receptor Suppresses Neuroinflammation and Neonatal Hypoxic-Ischemic Brain Injury. *Front. Neurol.* **12,** 607370 (2021).
47. Han, J., Fan, Y., Zhou, K., Zhu, K., Blomgren, K., Lund, H., Zhang, X.-M. & Harris, R. A. Underestimated Peripheral Effects Following Pharmacological and Conditional Genetic Microglial Depletion. *Int. J. Mol. Sci.* **21,** (2020).
48. Lund, H., Pieber, M., Parsa, R., Han, J., Grommisch, D., Ewing, E., Kular, L., Needhamsen, M., Espinosa, A., Nilsson, E., Överby, A. K., Butovsky, O., Jagodic, M., Zhang, X.-M. & Harris, R. A. Competitive repopulation of an empty microglial niche yields functionally distinct subsets of microglia-like cells. *Nat. Commun.* **9,** 4845 (2018).
49. Bruttger, J., Karram, K., Wörtge, S., Regen, T., Marini, F., Hoppmann, N., Klein, M., Blank, T., Yona, S., Wolf, Y., Mack, M., Pinteaux, E., Müller, W., Zipp, F., Binder, H., Bopp, T., Prinz, M., Jung, S. & Waisman, A. Genetic Cell Ablation Reveals Clusters of Local Self-Renewing Microglia in the Mammalian Central Nervous System. *Immunity* **43,** 92–106 (2015).
50. Rice, R. A., Spangenberg, E. E., Yamate-Morgan, H., Lee, R. J., Arora, R. P. S., Hernandez, M. X., Tenner, A. J., West, B. L. & Green, K. N. Elimination of Microglia Improves Functional Outcomes Following Extensive Neuronal Loss in the Hippocampus. *J. Neurosci.* **35,** 9977–9989 (2015).
51. Marzan, D. E., Brügger-Verdon, V., West, B. L., Liddelow, S., Samanta, J. & Salzer, J. L. Activated microglia drive demyelination via CSF1R signaling. *Glia* **69,** 1583–1604 (2021).
52. du Sert, N. P., Hurst, V., Ahluwalia, A., Alam, S., Avey, M. T., Baker, M., Browne, W. J., Clark, A., Cuthill, I. C., Dirnagl, U., Emerson, M., Garner, P., Holgate, S. T., Howells, D. W., Karp, N. A., Lazic, S. E., Lidster, K., MacCallum, C. J., Macleod, M., Pearl, E. J., Petersen, O. H., Rawle, F., Reynolds, P., Rooney, K., Sena, E. S., Silberberg, S. D., Steckler, T. & Wuerbel, H. The ARRIVE guidelines 2.0: updated guidelines

for reporting animal research. *BMJ Open Science* **4,** e100115 (2020).

53. Joanna M. Hill, Maria A. Lim, Madeleine M. Stone. in *Neuropeptide Techniques* (ed. Gozes, I.) 131–149 (Humana Press).
54. Rice, J. E., 3rd, Vannucci, R. C. & Brierley, J. B. The influence of immaturity on hypoxic-ischemic brain damage in the rat. *Ann. Neurol.* **9,** 131–141 (1981).
55. Vannucci, R. C. & Vannucci, S. J. A model of perinatal hypoxic-ischemic brain damage. *Ann. N. Y. Acad. Sci.* **835,** 234–249 (1997).
56. Ditelberg, J. S., Sheldon, R. A., Epstein, C. J. & Ferriero, D. M. Brain injury after perinatal hypoxia-ischemia is exacerbated in copper/zinc superoxide dismutase transgenic mice. *Pediatr. Res.* **39,** 204–208 (1996).
57. Yun, S., Reynolds, R. P., Petrof, I., White, A., Rivera, P. D., Segev, A., Gibson, A. D., Suarez, M., DeSalle, M. J., Ito, N., Mukherjee, S., Richardson, D. R., Kang, C. E., Ahrens-Nicklas, R. C., Soler, I., Chetkovich, D. M., Kourrich, S., Coulter, D. A. & Eisch, A. J. Stimulation of entorhinal cortex-dentate gyrus circuitry is antidepressive. *Nat. Med.* **24,** 658–666 (2018).
58. Lagace, D. C., Donovan, M. H., DeCarolis, N. A., Farnbauch, L. A., Malhotra, S., Berton, O., Nestler, E. J., Krishnan, V. & Eisch, A. J. Adult hippocampal neurogenesis is functionally important for stress-induced social avoidance. *Proc. Natl. Acad. Sci. U. S. A.* **107,** 4436–4441 (2010).
59. Tzakis, N. & Holahan, M. R. Social Memory and the Role of the Hippocampal CA2 Region. *Front. Behav. Neurosci.* **13,** 233 (2019).
60. Sheldon, R. A., Almli, L. & Ferriero, D. M. Copper/zinc superoxide dismutase transgenic brain in neonatal hypoxia-ischemia. *Methods Enzymol.* **353,** 389–397 (2002).
61. Ho, J., Tumkaya, T., Aryal, S., Choi, H. & Claridge-Chang, A. Moving beyond P values: data analysis with estimation graphics. *Nat. Methods* **16,** 565–566 (2019).
62. Lakens, D. Calculating and reporting effect sizes to facilitate cumulative science: a practical primer for t-tests and ANOVAs. *Front. Psychol.* **4,** 863 (2013).
63. Hellström Erkenstam, N., Smith, P. L. P., Fleiss, B., Nair, S., Svedin, P., Wang, W., Boström, M., Gressens, P., Hagberg, H., Brown, K. L., Sävman, K. & Mallard, C. Temporal Characterization of Microglia/Macrophage Phenotypes in a Mouse Model of Neonatal Hypoxic-Ischemic Brain Injury. *Front.*

Cell. Neurosci. **10,** 286 (2016).

64. Qiu, L., Zhu, C., Wang, X., Xu, F., Eriksson, P. S., Nilsson, M., Cooper-Kuhn, C. M., Kuhn, H. G. & Blomgren, K. Less neurogenesis and inflammation in the immature than in the juvenile brain after cerebral hypoxia-ischemia. *J. Cereb. Blood Flow Metab.* **27,** 785–794 (2007).
65. Shao, R., Sun, D., Hu, Y. & Cui, D. White matter injury in the neonatal hypoxic-ischemic brain and potential therapies targeting microglia. *J. Neurosci. Res.* **99,** 991–1008 (2021).
66. Guez-Barber, D., Colon, L. M., Raphael, D., Wragan, M. A., Yun, S. & Eisch, A. J. Female and male microglia are not different in the dentate gyrus of postnatal day 10 mice. *Neurosci. Lett.* **803,** 137171 (2023).
67. Jain, A., Huang, G. Z. & Woolley, C. S. Latent Sex Differences in Molecular Signaling That Underlies Excitatory Synaptic Potentiation in the Hippocampus. *J. Neurosci.* **39,** 1552–1565 (2019).
68. Lechner, C. R., McNally, M. A., St Pierre, M., Felling, R. J., Northington, F. J., Stafstrom, C. E. & Chavez-Valdez, R. Sex specific correlation between GABAergic disruption in the dorsal hippocampus and flurothyl seizure susceptibility after neonatal hypoxic-ischemic brain injury. *Neurobiol. Dis.* **148,** 105222 (2021).